Numerical Simulation of the Aerosol Particle Motion in Granular Filters with Solid and Porous Granules

Authors:

Olga V. Soloveva, Sergei A. Solovev, Ruzil R. Yafizov

Date Submitted: 2022-11-01

Keywords: granular filter, DEM, spherical granules, microporosity, Computational Fluid Dynamics, particle deposition efficiency, pressure drop, filter quality factor

Abstract:

In this work, a study was carried out to compare the filtering and hydrodynamic properties of granular filters with solid spherical granules and spherical granules with modifications in the form of micropores. We used the discrete element method (DEM) to construct the geometry of the filters. Models of granular filters with spherical granules with diameters of 3, 4, and 5 mm, and with porosity values of 0.439, 0.466, and 0.477, respectively, were created. The results of the numerical simulation are in good agreement with the experimental data of other authors. We created models of granular filters containing micropores with different porosity values (0.158?0.366) in order to study the micropores' effect on the aerosol motion. The study showed that micropores contribute to a decrease in hydrodynamic resistance and an increase in particle deposition efficiency. There is also a maximum limiting value of the granule microporosity for a given aerosol particle diameter when a further increase in microporosity leads to a decrease in the deposition efficiency.

Record Type: Published Article

Submitted To: LAPSE (Living Archive for Process Systems Engineering)

Citation (overall record, always the latest version): LAPSE:2022.0118
Citation (this specific file, latest version): LAPSE:2022.0118-1
Citation (this specific file, this version): LAPSE:2022.0118-1v1

DOI of Published Version: https://doi.org/10.3390/pr9020268

processes

MDPI

Article

Numerical Simulation of the Aerosol Particle Motion in Granular Filters with Solid and Porous Granules

Olga V. Soloveva [1,*], Sergei A. Solovev [2] and Ruzil R. Yafizov [1]

[1] Institute of Heart Power Engineering, Kazan State Power Engineering University, 420066 Kazan, Russia; ruzilyafizov@gmail.com
[2] Institute of Digital Technologies and Economics, Kazan State Power Engineering University, 420066 Kazan, Russia; solovev.sa@kgeu.ru
* Correspondence: solovyeva.ov@kgeu.ru

Abstract: In this work, a study was carried out to compare the filtering and hydrodynamic properties of granular filters with solid spherical granules and spherical granules with modifications in the form of micropores. We used the discrete element method (DEM) to construct the geometry of the filters. Models of granular filters with spherical granules with diameters of 3, 4, and 5 mm, and with porosity values of 0.439, 0.466, and 0.477, respectively, were created. The results of the numerical simulation are in good agreement with the experimental data of other authors. We created models of granular filters containing micropores with different porosity values (0.158–0.366) in order to study the micropores' effect on the aerosol motion. The study showed that micropores contribute to a decrease in hydrodynamic resistance and an increase in particle deposition efficiency. There is also a maximum limiting value of the granule microporosity for a given aerosol particle diameter when a further increase in microporosity leads to a decrease in the deposition efficiency.

Keywords: granular filter; DEM; spherical granules; microporosity; CFD; particle deposition efficiency; pressure drop; filter quality factor

Citation: Soloveva, O.V.; Solovev, S.A.; Yafizov, R.R. Numerical Simulation of the Aerosol Particle Motion in Granular Filters with Solid and Porous Granules. *Processes* **2021**, *9*, 268. https://doi.org/10.3390/pr9020268

Academic Editor: Hiroshi Mio
Received: 30 December 2020
Accepted: 27 January 2021
Published: 30 January 2021

1. Introduction

There are many types of filters, each of which performs its tasks and works under certain conditions [1,2]. Granular filters are the most widely used due to their versatility [3]. Depending on the granule size, shape, and the material from which it is made, it can be used to filter gases and liquids of various degrees of pollution and temperatures. Chemically-resistant materials in the chemical industry can also be used as catalysts [4–7]. Granular filters are cheap and simple to manufacture, and have a low flow resistance and large surface area compared to other types of filters.

Granular filters can be divided into several types; these are filters with moving, fixed, and fluidized beds. Fixed bed filters have a low particle deposition efficiency relative to other filters, and cannot operate without stopping. Fluidized bed filters have a low efficiency, but can run continuously. Moving bed filters have the highest particle deposition efficiency, and can be operated continuously [8]. Despite the low efficiency and the lack of the ability to work non-stop, the most common of these three types is the fixed bed filter; this is due to its greater reliability and availability, and the simplicity of modeling and predicting the filter parameters in it.

The calculation and prediction of filtration involve the various mechanisms due to which the deposition of particles occurs; these are interception, inertial deposition, diffusion, and gravitational and electrostatic attraction. Each of the mechanisms has a region of particle sizes within which it makes the main contribution to filtration. For example, diffusion and the gravity mechanism have noticeable effects if the particle diameter is less than 1 µm. In the range of particle sizes 1–50 µm, it is assumed that the main contribution is made by inertial deposition [9,10]. The mechanism of particle capture is closely related

to the parameters of the filters themselves—more precisely, to the granules, which are the filtering material—such as the method and porosity of the packing, the size, and shape of the granules; the hydrodynamic resistance of the filter depends on these parameters. The liquid or gas flow rate also makes a significant contribution to the filtration process [11–21].

Combining different granules in terms of particle deposition efficiency and pressure drop allows us to achieve better efficiency than the use of only one type of granules [22–24]. The authors of experimental work [25] substantiated the expediency of the use of a multilayer granular filter, which reduces the pressure drop by almost 50% while increasing the particle deposition efficiency by 3.23%. The experimental curves of the change in efficiency and pressure drop are given as a function of the filtration time for granule sizes of 3, 5, 8, 10 mm, and a filtration rate for a range of layers depths of 30, 60, 90, and 120 mm. All of these curves are also shown for the proposed multilayer filter model, consisting of a set of 3, 5, and 8 mm granules filled with equal layers.

Complex studies were carried out by Sahar Bakhshian and Muhammad Sahimi [26] to assess the effect of deformation on the morphology of porous media and the flow properties of packed beds. A wide range of parameters were analyzed before and after the deformation. Depending on the morphology of the porous structure, the opening and closing of the pores during deformation can lead to a significant change in permeability while changing parameters such as pore lengths, pore size distribution, and the porosity of the medium. The deformation and swelling of a porous medium when interacts with a liquid were studied in detail in work [27]. These studies are very important when considering the filtration of liquids in porous materials.

The authors of [28] numerically and experimentally investigated the effect of the depth of the filtering layer on pressure drop and particle deposition efficiency. They showed that an increase in the gas velocity increases the deposition efficiency for particles larger than 7 μm, which can be explained by their increasing inertia. It was also shown that the pressure drop changes linearly with the increasing layer depth. The deposition positions of a granular filter with random packing were determined in the work of the authors [29] for particles with sizes from 1 to 21 μm; the maximum area during deposition on granules is occupied by particles from 1 to 7 μm, and with an increase in particle size, the area of deposition decreases. The authors of the paper [30] investigated the filtration process in models of ordered body- and face-centered cubic packing granules. Parameters such as the particle deposition fraction—depending on the number of rows for two models of granule packing and pressure drop versus flow rate—were estimated. The behavior of the efficiency curves, represented as a function of the particle diameter, changes when the flow rate varies from 0.2 m/s to 1 m/s. In the indicated velocity range, the efficiency curves have a minimum at a particle size of 2 μm for the model's face-centered cubic packing, and at a particle size of 4 μm for the body-centered cubic packing model (except for the velocity value of 0.2 m/s). Later, the same authors [31] investigated a random packing of granules, which did not reveal an obvious minimum in the efficiency of the particle deposition in a similar range of calculated velocities for particles of 2 or 4 μm, which can be explained by the closeness of the last model to the real filter structure, and the absence of the influence of boundary conditions. In [32], heat transfer characteristics studies were added to the study of the deposition efficiency versus the particle diameter, and the pressure drop versus the bed depth.

An experimental study of various flow regimes within pores in a dense granular layer by the electrochemical method was carried out [33]. The Reynolds numbers in the study varied from 20 to 2200; the transition from a laminar to a turbulent flow regime was considered. The results demonstrate the effect of the tube diameter on the flow regime.

Studies of granular filters can be divided into several types. These are empirical, semi-empirical, and Computational Fluid Dynamics (CFD) modeling. Most filters in use today were invented in the early 2000s, and have not undergone any major changes. Their development was carried out based on semi-empirical dependencies, which were developed for a simple prediction. This method of application is universally impossible, as

each case requires its correlations, considering the peculiarities of the shape and packing of granules [34]. Experimental studies give accurate results, but this type of research is expensive, and does not allow us to see how the gas moves in the space between the granules, or how the deposition of particles of different sizes occurs. The use of numerical simulation technology allows us to consider in detail each parameter, predict the filter behavior under various conditions, and consider the movement of the particles inside the filter. The main problem of numerical simulation is the creation of a reliable model that will correspond to a real filter; compliance with this condition allows us to obtain data that correlate well with the experimental results. In most studies, in order to create a geometric model of a filter with randomly-packed granules, the Monte Carlo method is combined with the DEM (discrete element method) [35–38]. Computed tomography technologies are also used to create a geometric model from the images obtained. This method is well suited for making ready-made filter models, but it does not change its parameters.

Introduced by Cundall and Strack [39], the discrete element method (DEM) was widely used to simulate bulk media behavior and, in recent years, was actively used by researchers to simulate particle motion in granular filters. This method offers the possibility of deeply understanding the motion of particles of different shapes in granular filter models. Shire and O'Sullivan, in their work [40], analyzed the constriction size distribution on models of granular filters that were created using DEM. The work [41] is devoted to the study of the motion of a wet granular layer. The breakage phenomenon of particles with sharp edges is considered in the article [42] through the combination of the discrete element method (DEM) and the finite element method (FEM). The work [43] is devoted to the study of the particle's shape's influence on the behavior of the granular layer. Experiments were carried out with rice grains and glass beads on an unbaffled rotary drum using a high-speed camera, the results of which were repeated through numerical simulation using DEM. The authors of [44] estimated the change in permeability during the deposition of large- and small-sized particles in a porous medium consisting of a disordered packing of spheres by combining DEM and the network model.

In their investigations, the authors of work [45] used the DEM method to determine the particle collision frequency on the surface of particles on any plane perpendicular to the flow direction. Although He et al. [46] argued that this method is computationally-demanding in terms of calculations, Guo et al. [47] observed that some particle-scale quantities—such as the position, orientation, and contact force—could be obtained by implementing the DEM simulation technique. Moreover, the authors of work [48] applied a 3D geometric modeling assumption to illustrate a decrease in the computational efforts based on specific particle dispositions in granular filters.

In recent years, the formation of particle piles was studied based on diverse granular shapes. The wedge sequence and the layered sequence were commonly used to assemble a pile. While, in the first method, a pile is formed from a particle point source, in the second, a pile is formed by dropping a layer of particles from a specific height of less than one particle diameter [49–51]. Many authors have investigated the relationship between stress distribution and particle sizes in granular models. Matuttis et al. [50] analyzed the particle deposition of a circular and a polygonal shape. On the other hand, Zhu et al. [52] observed that particle elongation is possible with a pressure drop at the bottom of a pile. Furthermore, the authors of the paper [53] focused on the study of the pile formation of ellipsoidal granules.

Coupled with the computational fluid dynamics solver (CFD), the discrete element method (DEM) has become particularly attractive for the simulation of large-scale industrial processes due to excellent mass and heat transfer attributes that result from its application [54].

This paper presents a CFD simulation of the motion of aerosol particles in granular filter models created by DEM for spherical granules with a diameter of 3, 4, and 5 mm. Parameters such as the pressure drop, particle deposition efficiency, and filter quality factor were investigated. It was suggested that it is possible to use filters with porous granules

to reduce the pressure drop and increase the particle deposition efficiency. Studies of the influence of the granule micro-porosity on the above-mentioned parameters in the granular layer were carried out. In general, porous granules can be widely used in practice.

2. Problem Formulation and Solution Method

2.1. Filter Model

When choosing filters, the question arises as to which filter is the best for a given technological cycle. Current granular filters can have complex internal structures, where gas dynamics is the main contributor to particle deposition efficiency. The different geometries of the internal structure of filters affect the flow field and, consequently, the efficiency of particle deposition. This work aimed to determine the granular filter parameters (granule size, porosity, microporosity) that make the most significant contribution to the change in the deposition efficiency of aerosol particles, the resistance, and the filter quality factor.

For submicron-sized particles, the predominant deposition mechanism in porous structures is inertial deposition. For granular filters, the actual granule size is in the range of 1–10 mm. For example, in works [28,29,32], experimental and numerical studies of the operation of granular filters with granule sizes of 5, 6, and 10 mm were carried out. In works [30,31,55], the operation of a filter with granules with a diameter of 5 mm was investigated. In works [56,57], filters with a granule diameter of 1–5 mm were selected. In [25], experimental studies were carried out for filters with granule diameters of 3, 5, 8, and 10 mm. We made a numerical simulation for a set of models of granular filters with granule diameters of $d_g = 3$, $d_g = 4$, and $d_g = 5$ mm. The discrete element method (DEM) was used to create the geometries in YADE [58]. An example of the creation of a granular filter bed is shown in Figure 1. The figure shows four pictures of the process of pouring granules into the cylinder at different time intervals: 0.15 s, 0.21 s, 0.65 s, and 1.0 s. In the calculations, the density of the granules is 1800 kg/m^3. Due to the random arrangement of the granules in the filter package, the calculations were averaged for five different geometries, which were created with similar physical parameters to eliminate errors.

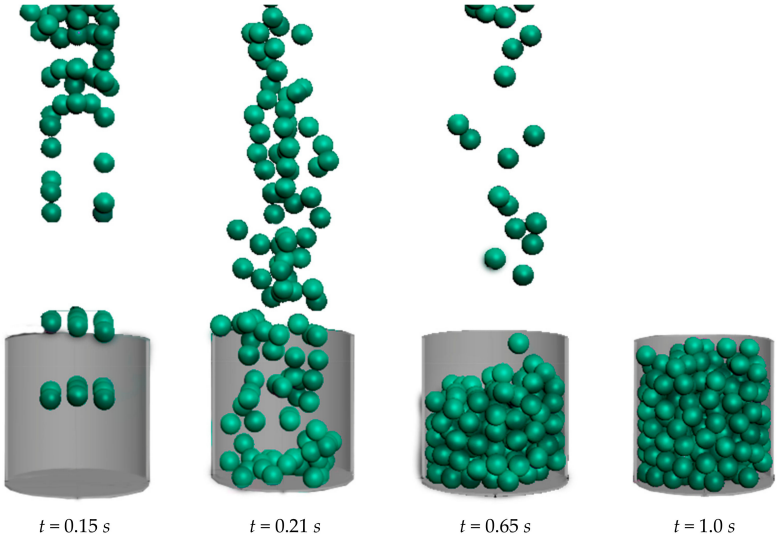

Figure 1. An example of a filter model created by pouring spherical granules into a cylindrical area; the dynamics are in the time interval t = 0.15–1.0 s.

For the calculations, a cylindrical area with a diameter of 20 mm and a length of 20 mm, filled with spherical granules, was selected (Figure 2). The number of granules was from 221 to 235 units for the case of $d_g = 3$ mm, from 98 to 103 units for the case of $d_g = 4$ mm, and from 45 to 47 units for the case of $d_g = 5$ mm. For a small size mm, the number of granules is significantly larger. In this case, the deviation in the number of granules relative to the average value is from 4.4% ($d_g = 5$ mm) to 6.3% ($d_g = 3$ mm).

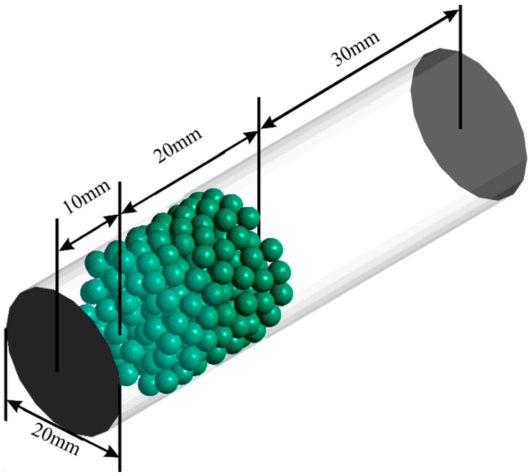

Figure 2. Filter model: solid spherical granules (d_g = 3 mm, ε = 0.439).

An inlet section, 10 mm long, was located before packing the granules to form a gas flow, and after the granules, there was an outlet part 40 mm long. The parameters of the models created for the study are presented in Table 1.

Table 1. Parameters of the spherical granule packing models used for the calculations.

Granule Diameter d_g, mm	Tube to Granule Diameter Ratio d_t/d_g	Porosity ε	Porosity, Calculated by the Formula (1) $\varepsilon_{(1)}$
3	6.67	0.439	0.418
4	5	0.466	0.436
5	4	0.477	0.455

We verified the constructed models by comparing the porosity parameters of the bed of spherical granules created by the DEM method with the following formula [59]:

$$\varepsilon = 0.390 + \frac{1.740}{\left(\frac{d_t}{d_g} + 1.140\right)^2}, \quad (1)$$

where d_t is the tube diameter. Calculations using the Formula (1) are also presented in Table 1. In this work, we calculate the porosity of the granule layer, limiting the considered volume from below and from above by the boundary point of the presence of the granule. Therefore, the calculated values of porosity ε are less than those calculated by the formula $\varepsilon_{(1)}$.

From Formula (1), it follows that the porosity depends on the diameter of the area into which the granules are poured. Regardless of the granule size, with a large increase in the size of the region ($d_t/d_g > 15$), the porosity tends to a value of 0.39 for the dense packing of the spheres. A strong influence in the value of the porosity of the packing of the spheres is observed at $d_t/d_g < 10$. This paper does not consider the effect of the tube size on the efficiency of the filtering layer of granules. We will investigate the effect of the granule diameter, as well as the presence of micropores, on the performance of a granular filter for a fixed area.

2.2. Mathematical Formulation

We calculated the gas flow (airflow) based on the solution of the equations for the conservation of mass and the conservation of momentum for a stationary problem.

Mass conservation equation:

$$\nabla \cdot \vec{V} = 0, \quad (2)$$

where $\vec{V}$ is the gas velocity.

The momentum conservation equation:

$$\rho\vec{V}\cdot\nabla\vec{V} = -\nabla P + \mu\Delta\vec{V}, \tag{3}$$

where ρ is the gas density, P is the pressure, and μ is the gas dynamic viscosity coefficient.

The trajectories of aerosol particle motion were calculated in the found field of the gas velocities based on Newton's law for single-particle motion:

$$\begin{aligned} \frac{d\vec{R}_p}{dt} &= \vec{V}_p, \\ \frac{d\vec{V}_p}{dt} &= \frac{\vec{V}-\vec{V}_p}{\tau}, \end{aligned} \tag{4}$$

where $\vec{R}_p$ is the vector of the coordinates of the aerosol particle, $\vec{V}_p$ is the velocity of the aerosol particle, and τ is the relaxation time of the particle, calculated as in [60]:

$$\tau = \frac{\rho_p d_p^2}{18\mu}, \tag{5}$$

where ρ_p is the particle density used in calculations 1500 kg/m^3, and d_p is the aerosol particle diameter.

It is assumed that the aerosol particles that reach the filter surface are deposited on it. In this case, the captured particles are removed from the computational domain [61,62].

At the inlet boundary of the computational domain is set the value of the mass gas flow rate; at the outlet boundary is set the value of atmospheric pressure; other boundaries were taken by default as impermeable walls. The solution to the problem of stationary gas flow (2) and (3) was obtained by the finite volume method in the CFD package ANSYS Fluent (v. 19.2). The geometry of the porous region is such that, even at low flow rates, the active mixing of the flow occurs, and a turbulent flow regime is observed. The average flow rate accepted in the calculation of the particle trajectories was 1 m/s, which corresponds to a turbulent flow regime. We decided to use direct numerical simulation (DNS) in the calculations. The number of elements of the grid division of the region in the calculations is 12,000,000.

After calculating the gas flow field, we calculated the particle motion using Formulas (4) and (5) in ANSYS Fluent (v. 19.2). Spherical particles start at the computational domain's entrance and their direction is normal to the boundary. Then, the particles move against the background of the calculated gas field; for the presented calculations, we started with 30,000 particles. Only the trajectory of motion of the particle center was considered; the density and diameter of the particle affect the inertia and contribute to the deposition, with a sharp deviation of the flow near a solid surface. The particles that reached the surface of the filter granules were considered settled, and were excluded from the further calculation of the trajectories' motion. The particles that reached the surface of the tube were reflected, and their further movement was calculated.

3. Results

3.1. Numerical Simulation of the Aerosol Motion in a Granular Filter with Solid Spherical Granules

The numerical calculations were compared with the data of the semi-empirical dependence for the pressure drop ΔP relative to length L of a granular medium [63], in order to assess the correctness of the gas flow model:

$$\frac{\Delta P}{L} = 150\frac{\mu(1-\varepsilon)^2 V}{d_g^2\varepsilon^3} + 1.75\frac{\rho(1-\varepsilon)V^2}{d_g\varepsilon^3}, \tag{6}$$

In [64], a formula was proposed to take into account the tube diameter:

$$\frac{\Delta P}{L} = 154 A_w^2 \frac{\mu(1-\varepsilon)^2 V}{d_g^2 \varepsilon^3} + \frac{A_w}{B_w} \frac{\rho(1-\varepsilon)V^2}{d_g \varepsilon^3},$$
$$A_w = 1 + \frac{2}{3}\frac{d_g}{d_t}(1-\varepsilon), \quad (7)$$
$$B_w = \left(1.15\frac{d_g}{d_t} + 0.87\right)^2,$$

Figure 3 shows a comparison of the numerical simulation results and the application of semi-empirical Formulas (6) and (7) for the pressure drop. The graphs show that the pressure drop curves correlate well with each other for all three granule diameters: 3, 4, and 5 mm. Formula (7) was designed to consider the effect of the tube walls near the granules on the pressure drop. In [64], the existing models for the calculation of the pressure drop are considered in detail, and the difference in the value of the pressure drop for an unrestricted layer of granules and a layer of granules enclosed in a narrow tube is described. In our case, despite the presence of a tube, the graphs of the calculated pressure drop are closer to the curve calculated by Formula (6) for an unlimited layer of granules than to the curve calculated by Formula (7) for a limited layer of granules. We believe that this is because a layer of granules of small thickness was considered, and in the filter zone, there was no time to form a near-wall layer sufficient to influence the pressure drop. In [32], experimental and numerical calculations of the pressure drop for a granular layer in a confined tube are performed, which show good agreement with the calculations by Formula (6).

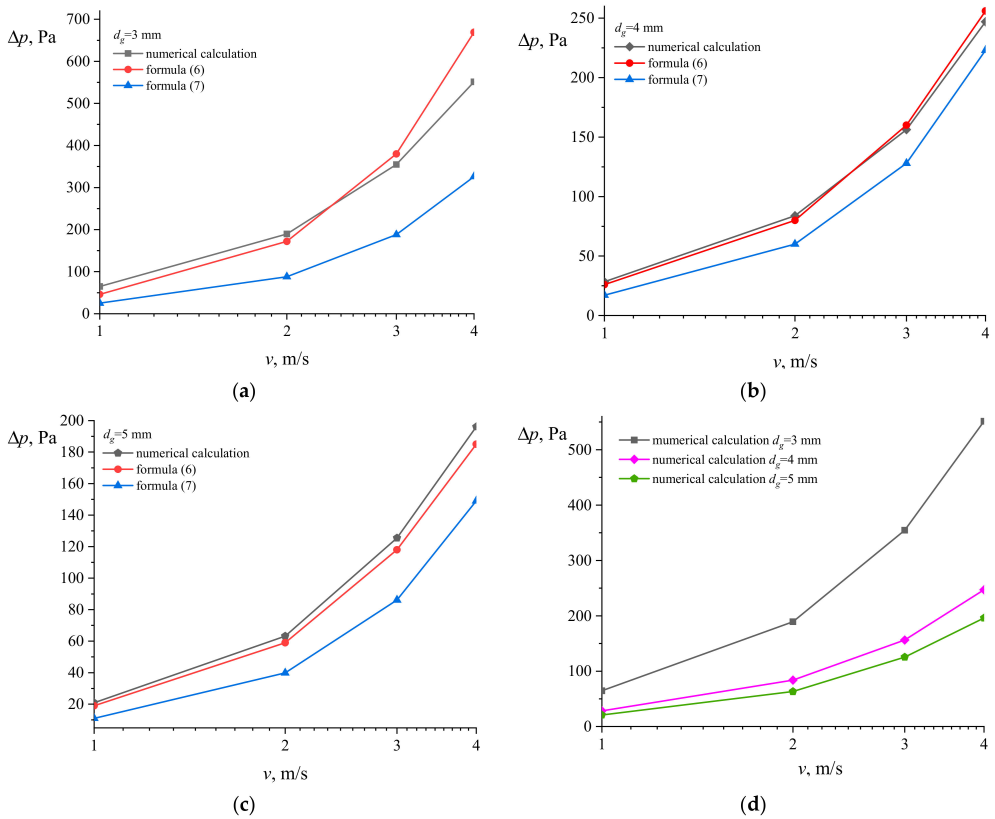

Figure 3. Dependence of the pressure drop on the gas flow rate: (**a**) $d_g = 3$ mm; (**b**) $d_g = 4$ mm; (**c**) $d_g = 5$ mm; (**d**) comparison of the numerical simulation results.

Furthermore, we studied the particle deposition efficiency, which is defined as the ratio of the number of particles deposited on the filter surface to the total number of particles that started at the inlet boundary, which is given as

$$E = \frac{n_p^{trap}}{n_p^{total}}, \tag{8}$$

where n_p^{trap} is the number of deposited particles, and n_p^{total} is the total number of starting particles.

Figure 4 shows an example of the particle trajectories in a filter for a particle diameter of $d_p = 1.8 \cdot 10^{-6}$ m.

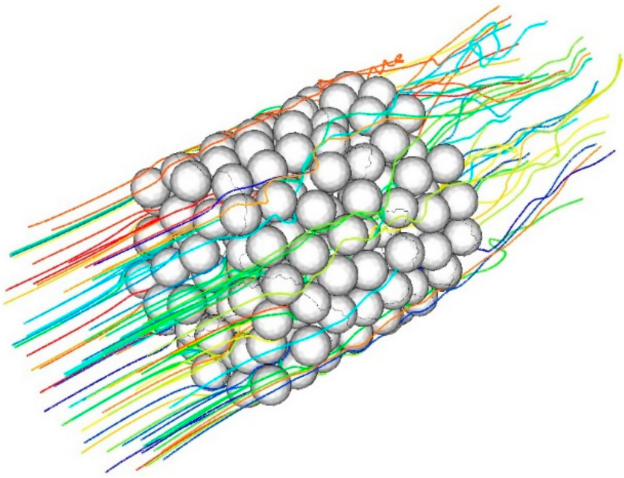

Figure 4. Particle trajectories in the filter model.

We performed a comparative calculation to verify our research. In studies [28,29], the filtration efficiency curve for a granular filter with a granule diameter of $d_g = 10$ mm is presented. We constructed a cylindrical region with a granular filter, as in [29], calculated the gas movement at a similar velocity of 0.345 m/s, and calculated the motion and deposition of aerosol particles with a diameter of 1 µm to 21 µm. The results are presented in Figure 5. The result of our calculation is in good agreement with the results of the experimental studies.

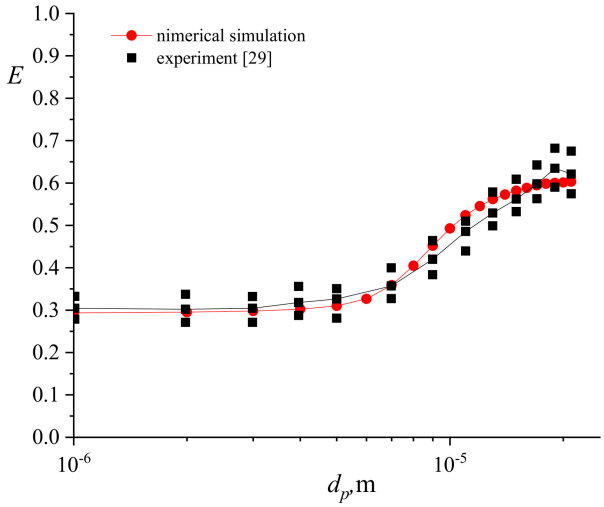

Figure 5. Comparison of the filtration efficiency of a granular filter with the experimental data [29].

Figure 6a shows the results of a study of the particle deposition efficiency for the filter models with spherical granules for various values of the porosity of the medium. Calculations of the efficiency were carried out for all of the constructed geometries, and thus, for each value of the granule diameter, we averaged the results over five calculations. We can see that the filter with $d_g = 3$ mm granules has the best efficiency among the cases of our calculations. In this case, the largest scatter in the results (up to 8.6%) can also be observed for granules with a diameter of 3 mm. For packages of granules with a diameter of 5 mm, the scatter of the results is not large (up to 2.35%).

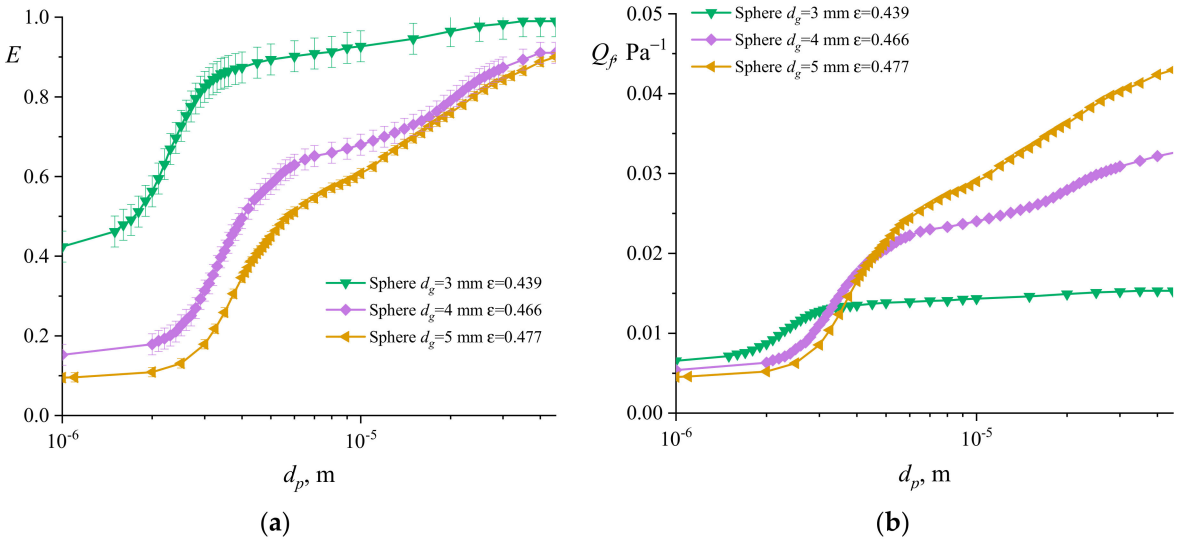

Figure 6. Dependence on the particle diameter: (**a**) particle deposition efficiency; (**b**) filter quality factor.

Let us consider the filter quality factor. In experimental studies [65], where the number of particles that are not settled on the filter is estimated, one can find the expression $Q_f = -\ln(C_{out}/C_{in})/\Delta P$, where C_{out} and C_{in} are the concentrations of particles at the outlet and inlet of the filter, respectively. In our research, we calculated the filter quality factor as the ratio of the particle deposition efficiency to the pressure drop characterizing the hydrodynamic resistance of the medium.

$$Q_f = \frac{E}{\Delta P}. \tag{9}$$

Figure 6b shows the calculation results. For small particles (up to $d_p = 3 \cdot 10^{-6}$ m), a filter with spherical granules with a diameter of $d_g = 3$ mm has the highest quality factor among the cases of our calculations. The largest deviation on the graphs is for deposition efficiency. As the particle diameter increases, its quality factor curve is lower than that of all of the other granule models. The model with granules with a diameter of $d_g = 5$ mm has the highest quality factor for larger particle sizes. This effect is explained by a decrease in the deposition efficiency value deviation with an increase in the diameter of the aerosol particles. Obviously, with a large value of the particle diameter, the deposition efficiency will tend to 1 (provided no transparency and holes in the filter), at which point the pressure drop will completely determine the filter quality.

3.2. Numerical Simulation of the Aerosol Motion in a Granular Filter with Porous Spherical Granules

Furthermore, we studied the possibility of improving the filtering properties of granular filters with spherical granules. For this, we modified the filter with porous granules with a diameter of $d_g = 5$ mm (Figure 7). The micropore diameter was $d_{mic} = 1.9$ mm. By

increasing and decreasing the distance between the micropores, we controlled the porosity value. The porosity parameters of the created models are presented in Table 2.

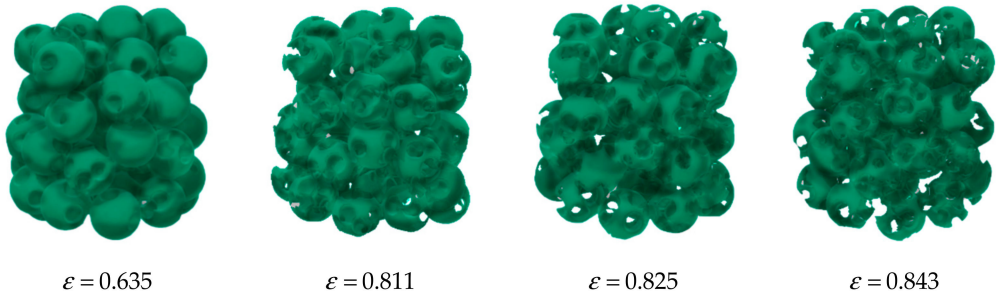

Figure 7. Examples of a packing model for spheres with micropores.

Table 2. Porosity value of the created models.

Macroporosity ε_{mac}	Microporosity ε_{mic}	Total Porosity ε
0.477	0.073	0.550
	0.158	0.635
	0.273	0.750
	0.334	0.811
	0.348	0.825
	0.366	0.843

The addition of micropores entails an increase in the mesh elements required for the calculations. As such, if for the case of solid spheres there were 12,000,000 elements in the mesh, then for the case of total porosity $\varepsilon = 0.635$ the number of elements is about 14,000,000, and for the case of total porosity $\varepsilon = 0.825$ the number of elements is about 16,000,000.

Figure 8 shows the results of a study of the particle deposition efficiency for filter models with modified granules compared to the model without micropores. It is obvious that the addition of micropores affects the behavior of the movement of the liquid and aerosol particles inside the granular filter. Particles, moving with the gas flow, can penetrate into the granules and settle during their movement in the internally-developed porous structure.

Figure 8 shows that with the modification of a granular filter with micropores, an increase in particle deposition efficiency is observed in the entire range of particle sizes, which ranges from 10% to 25%. In this case, with a slight increase in porosity ($\varepsilon = 0.55$, $\varepsilon = 0.635$), the deposition efficiency curves qualitatively repeat the character of the curve, as for a bed of granules without micropores. Then, with an increase in porosity ($\varepsilon = 0.75$), the character of the curve begins to change. Models of filters with different total porosity values show different results for different ranges of values of particle diameters. Thus, a filter with total porosity $\varepsilon = 0.635$ demonstrates an efficiency of particle deposition higher than others by 5–8% in the area of particles up to $2 \cdot 10^{-6}$ m, and a further increase in porosity leads to a decrease in efficiency. Then, we can observe the intersection of the curves of the aerosol particle deposition efficiency for different porosity values. In the area of large particles, filters with total porosity of $\varepsilon = 0.811$, $\varepsilon = 0.825$ and $\varepsilon = 0.843$ work better. A structure with porosity $\varepsilon = 0.825$ has the most excellent efficiency, and a further increase in porosity also leads to a decrease in efficiency. Thus, small and large particles have their own porosity, which determines the maximum deposition efficiency.

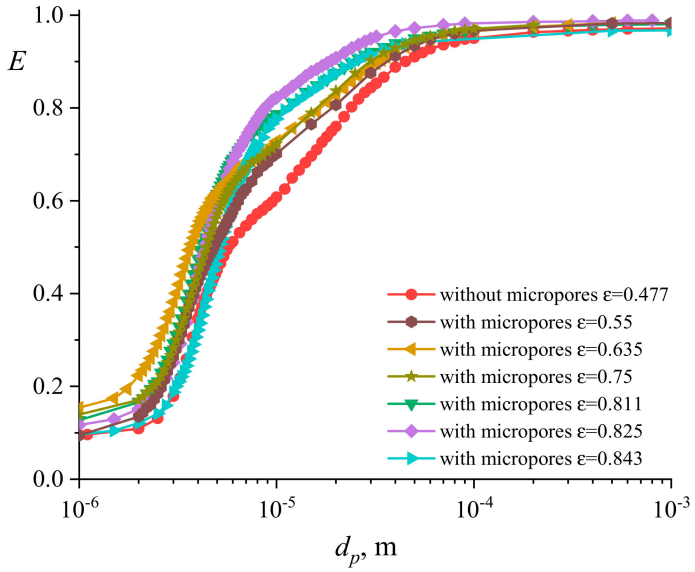

Figure 8. Dependence of the particle deposition efficiency on the particle diameter for models with and without micropores.

Obviously, the addition of multiple pores should increase the total surface area of the bed. However, too many pores can reduce the surface area of the bed. Figure 9a shows the calculated dependence of the bed area on porosity. The largest surface area is observed for the porosity range $\varepsilon = 0.635 - 0.811$. Here the analysis of the averaged efficiency curves is carried out; the analysis of the scatter of the results for specific values of the diameter of the aerosol particles is discussed below. This conclusion is valid for the special cases of geometric characteristics that we have chosen for the calculations in this study.

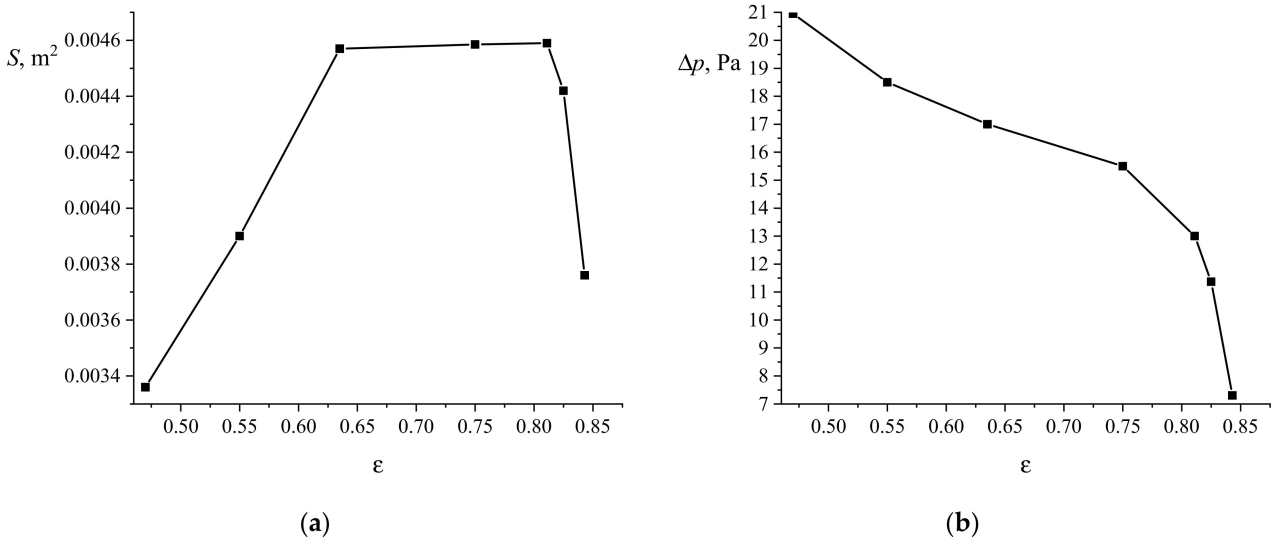

Figure 9. The parameters of the granular bed depend on the flow rate: (**a**) bed area; (**b**) pressure drop.

Figure 9b shows a graph of pressure drop versus flow rate. The structure with the highest porosity has the lowest pressure drop. The addition of micropores helps to reduce the flow resistance of the filter.

Figure 10 shows the dependence of the filter quality factor on the particle diameter. The original filter model without micropores has the minimum value of the quality factor. This result is due to the combination of the study results of the particle deposition efficiency

and pressure drop; in both indicators, the model without micropores is inferior to the models with micropores. Since the pressure drop makes the main contribution to the quality factor, the structure with the highest porosity value $\varepsilon = 0.843$, which corresponds to the lowest pressure drop, has the highest performance.

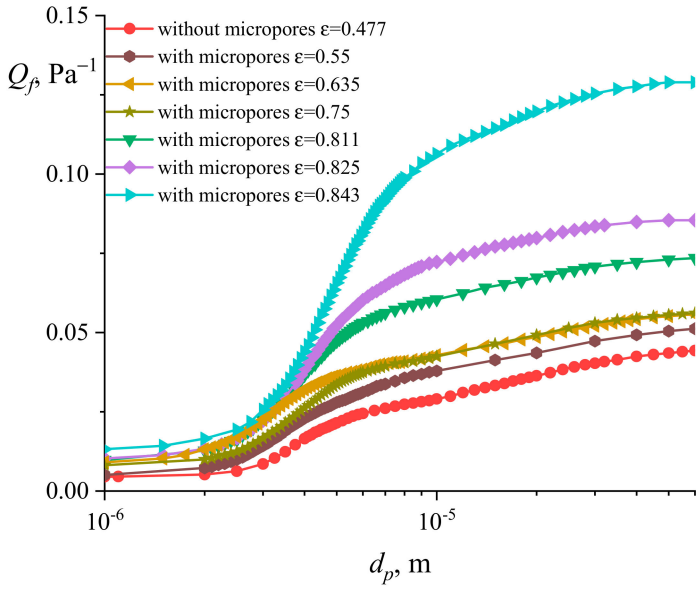

Figure 10. Changes in the quality factor versus the particle diameter for a filter with microporous granules.

The calculation results show that it is impossible to single out a filter with one porosity value as the most effective in a wide range of aerosol particle sizes. Next, we considered the values of the deposition efficiency of aerosol particles and the filter quality factor for particle size values $d_p = 1$ µm, $d_p = 4$ µm, $d_p = 10$ µm, and $d_p = 30$ µm. Figure 11 shows the results.

For small particle diameters, the most excellent efficiency is achieved for porosity $\varepsilon = 0.635$, when the filter has the largest surface area. For the deposition of small, weakly-inertial particles, the curvature of the rotation of the streamline of the carrier gas flow near the filter surface plays an important role. The porosity $\varepsilon = 0.635$ provides a large surface area due to the hollow spherical inclusions inside the granule, with several connecting channels. Small particles trapped inside the porous granule along with the gas are more likely to settle inside the micropore. A further increase in porosity leads to the destruction of the granule's surface, so the total surface area remains almost unchanged. Many micropores and connecting holes inside the granule do not contribute to the capture of small particles, which deviate slightly from the gas flow lines. At the same time, we found that the maximum value of the filter surface area does not provide the greatest value of the large particle deposition efficiency. The highest efficiency is determined at $\varepsilon = 0.825$. A further increase in porosity leads to the formation of straight, open channels in the filter, and particle motion without contact with the granules.

Figure 11a also shows the scatter bars for the calculation of the deposition efficiency of aerosol particles. For each value of the total porosity, we created five sets of granule packs, as for solid spheres. For each constructed filter geometry, the calculation of the movement and deposition of the aerosol particles was carried out. We observed the greatest scatter of results (up to 7%) in our calculations for the porosity value $\varepsilon = 0.635$. The scatter of results decreases both with a decrease in porosity until a solid sphere is reached, and with a strong increase in porosity. This may be because, for $\varepsilon = 0.635$, the number of pores in a separate granule is small (see Figure 7), and their position of the granule in space can have a strong effect on the movement of gas and aerosol particles in the filter. With a high porosity of

$\varepsilon = 0.843$, each granule has a highly-developed internal structure, such that the position of the granules in the filter layer does not have a critical effect on the filtering properties, and the filter itself becomes closer to an open cell foam. At the same time, the scatter of the results is less than 1%.

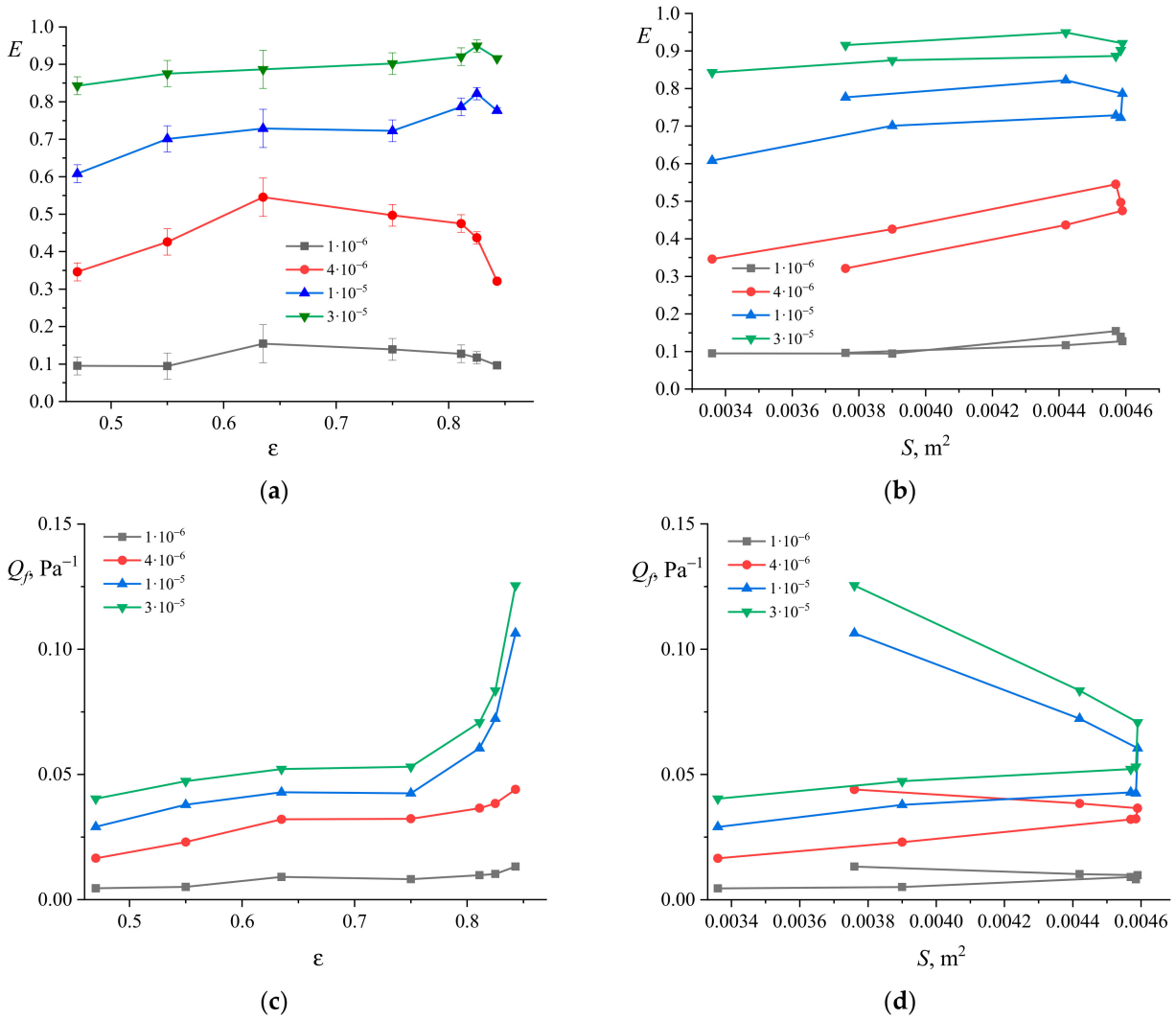

Figure 11. Dependence of the filter characteristics for particle size values d_p = 1 µm, d_p = 4 µm, d_p = 10 µm and d_p = 30 µm: (**a**) particle deposition efficiency on porosity; (**b**) particle deposition efficiency on surface area; (**c**) filter quality on porosity; (**d**) filter quality on surface area.

Considering the scatter of the results for the selected particle diameter $d_p = 1$ µm and $d_p = 30$ µm, we can say that, for the filter parameters used, the deposition efficiency of the aerosol particles is almost independent of the porosity of the granules. The main attention here can be paid to the reduction of the aerodynamic drag of the filter. For the case of $d_p = 4$ µm, the porosity value $\varepsilon = 0.635$ provides an advantage over filters with other porosity values in particle deposition efficiency, even taking into account the larger scatter of the calculation results. This conclusion was obtained for the specific case considered, but these results could be useful in studies to optimize the operation of granular filters.

4. Conclusions

We carried out a numerical simulation of aerosol motion in models of granular filters with granules of various sizes, i.e., 3, 4, and 5 mm in diameter. We investigates the particle deposition efficiency over a wide range of sizes and aerodynamic drag as a pressure drop.

The $d_g = 3$ mm granule filter has the highest particle deposition efficiency, but also the highest resistance. The analysis of the filter quality factor parameter made it possible to divide the scale of the aerosol particle diameters into areas in which, for small particles, it is preferable to use a filter with a denser packing of granules ($d_g = 3$ mm), and for large particles, the deposition efficiency values are close, and its aerodynamic resistance determines the filter quality.

The analysis of the calculation results for a filter modified by micropores with spherical granules with a diameter of $d_g = 5$ mm shows that, for almost all of the models with any microporosity of the granules, there is an increase in the particle deposition relative to the original model. The particle deposition efficiency does not change much with the addition of microporosity to the granules for very small and very large particles. For medium-sized particles, the optimum porosity value can be determined, i.e., the value at which the highest deposition efficiency is achieved. In our calculations for the case of $d_p = 4$ μm, we obtained the optimal value of porosity $\varepsilon = 0.635$, for the case of $d_p = 30$ μm—$\varepsilon = 0.825$. At the same time, by adding micropores, we can significantly reduce the aerodynamic drag of the filter. For all of the considered cases, the value of the filter quality factor reaches the highest value at the maximum value of the total porosity of the granule layer.

In this work, the presented results and conclusions refer to a specific filter geometry. These results may be of interest for the design of new granular filters, and the optimization of the operation of existing granular filters. We foresee further research in this direction in the tasks of the analysis of the effect of micropore size, granule size, and filter size on the performance of granular filters.

Author Contributions: Conceptualization, O.V.S.; methodology, O.V.S., S.A.S. and R.R.Y.; software, O.V.S., R.R.Y.; validation, O.V.S., S.A.S. and R.R.Y.; formal analysis, O.V.S., R.R.Y.; investigation, O.V.S., S.A.S.; data curation, R.R.Y.; Writing—Original draft preparation, O.V.S., R.R.Y.; Writing—Review and editing, O.V.S., S.A.S.; visualization, R.R.Y.; supervision, O.V.S.; project administration, O.V.S.; funding acquisition, O.V.S. All authors have read and agreed to the published version of the manuscript.

Funding: This research was funded by the Russian Science Foundation, grant number 19-71-00100.

Institutional Review Board Statement: Not applicable.

Informed Consent Statement: Not applicable.

Data Availability Statement: Data sharing not applicable.

Conflicts of Interest: The authors declare no conflict of interest.

References

1. Jaeger, H.M.; Nagel, S.R.; Behringer, R.P. Granular solids, liquids, and gases. *Rev. Mod. Phys.* **1996**, *68*, 1259–1273. [CrossRef]
2. Cai, J.; Dong, H.; Fu, W. Study on Particle Flow in Shaft Moving Beds. *J. Northeast. Univ. Nat. Sci.* **2007**, *28*, 1599–1603.
3. Tien, C.; Ramarao, B.V. Macroscopic description of fixed-bed granular filtration. In *Granular Filtration of Aerosols and Hydrosols*; Elsevier: Amsterdam, The Netherlands, 1989; pp. 17–47.
4. El-Hedok, I.A.; Whitmer, L.; Brown, R.C. The influence of granular flow rate on the performance of a moving bed granular filter. *Powder Technol.* **2011**, *214*, 69–76. [CrossRef]
5. Altmann, J.; Rehfeld, D.; Träder, K.; Sperlich, A.; Jekel, M. Combination of granular activated carbon adsorption and deep-bed filtration as a single advanced wastewater treatment step for organic micropollutant and phosphorus removal. *Water Res.* **2016**, *92*, 131–139. [CrossRef] [PubMed]
6. Hsu, C.J.; Hsiau, S.S. A study of filtration performance in a cross-flow moving granular bed filter: The influence of gas flow uniformity. *Powder Technol.* **2015**, *274*, 20–27. [CrossRef]
7. Hsu, C.J.; Hsiau, S.S.; Chen, Y.S.; Smid, J. Investigation of the gas inlet velocity distribution in a fixed granular bed filter. *Adv. Powder Technol.* **2010**, *21*, 614–622. [CrossRef]
8. Xiao, G.; Wang, X.; Zhang, J.; Ni, M.; Gao, X.; Luo, Z.; Cen, K. Granular bed filter: A promising technology for hot gas clean-up. *Powder Technol.* **2013**, *244*, 93–99. [CrossRef]
9. Gutfinger, C.; Tardos, G.I. Theoretical and experimental investigation on granular bed dust filters. *Atmos. Environ.* **1979**, *13*, 853–867. [CrossRef]
10. Brown, R.C.; Shi, H.; Colver, G.; Soo, S.C. Similitude study of a moving bed granular filter. *Powder Technol.* **2003**, *138*, 201–210.

11. Çarpinlioğlu, M.Ö.; Özahi, E. A simplified correlation for fixed bed pressure drop. *Powder Technol.* **2008**, *187*, 94–101.
12. Kuo, Y.M.; Huang, S.H.; Lin, W.Y.; Hsiao, M.F.; Chen, C.C. Filtration and loading characteristics of granular bed filters. *J. Aerosol Sci.* **2010**, *41*, 223–229. [CrossRef]
13. Solovev, S.A.; Soloveva, O.V.; Popkova, O.S. Numerical simulation of the motion of aerosol particles in open cell foam materials. *Russ. J. Phys. Chem. A* **2018**, *92*, 601–604. [CrossRef]
14. Zaripov, S.K.; Soloveva, O.V.; Skvortsov, E.V. Analytical model of the transport of aerosol particles in a circular hole inside a porous medium. *Transp. Porous Media* **2015**, *107*, 141–151. [CrossRef]
15. Soloveva, O.V.; Solovev, S.A.; Khusainov, R.R. Evaluation of the efficiency of prefilter models using numerical simulation. *J. Phys. Conf. Ser.* **2019**, *1399*, 022059. [CrossRef]
16. Soloveva, O.V.; Solovev, S.A.; Yafizov, R.R. Study of the influence of the add of micropores on filtering characteristics of high porous structures. *Ecol. Ind. Russ.* **2020**, *24*, 39–43. [CrossRef]
17. Soloveva, O. Study of aerosol motion in granular and foam filters with equal porosity of the structure. *Adv. Intell. Syst. Comput.* **2021**, *1259*, 638–649.
18. Soloveva, O.; Solovev, S.; Khusainov, R.; Yafizov, R. Mathematical modelling of heat transfer in open cell foam of different porosities. *Adv. Intell. Syst. Comput.* **2021**, *1259*, 371–382.
19. Choi, J.H.; Choi, K.B.; Kim, P.; Shun, D.W.; Kim, S.D. The effect of temperature on particle entrainment rate in a gas fluidized bed. *Powder Technol.* **1997**, *92*, 127–133. [CrossRef]
20. Wey, M.Y.; Chen, K.H.; Liu, K.Y. The effect of ash and filter media characteristics on particle filtration efficiency in fluidized bed. *J. Hazard. Mater.* **2005**, *121*, 175–181. [CrossRef]
21. Liu, K.Y.; Wey, M.Y. Filtration of nano-particles by a gas–solid fluidized bed. *J. Hazard. Mater.* **2007**, *147*, 618–624. [CrossRef]
22. Tian, S.R.; Yang, G.H.; Li, Z.; Shi, K.Y.; Ding, G.Z.; Hu, F.X. Cascade filtration properties of a dual-layer granular bed filter. *Powder Technol.* **2016**, *301*, 545–556. [CrossRef]
23. Paenpong, C.; Pattiya, A. Filtration of fast pyrolysis char fines with a cross-flow moving-bed granular filter. *Powder Technol.* **2013**, *245*, 233–240. [CrossRef]
24. Yang, G.; Zhou, J. Experimental study on a new dual-layer granular bed filter for removing particulates. *J. China Univ. Min. Technol.* **2007**, *17*, 201–204. [CrossRef]
25. Yu, Y.S.; Tao, Y.B.; Ma, Z.; He, Y.L. Experimental study and optimization on filtration and fluid flow performance of a granular bed filter. *Powder Technol.* **2018**, *333*, 449–457. [CrossRef]
26. Bakhshian, S.; Sahimi, M. Computer simulation of the effect of deformation on the morphology and flow properties of porous media. *Phys. Rev. E* **2016**, *94*, 042903. [CrossRef]
27. Bakhshian, S.; Sahimi, M. Adsorption-induced swelling of porous media. *Int. J. Greenh. Gas Control* **2017**, *57*, 1–13. [CrossRef]
28. Guan, L.; Gu, Z.; Yuan, Z.; Yang, L.; Zhong, W.; Wu, Y.; Sun, S. Numerical study on the penetration of ash particles in a three-dimensional randomly packed granular filter. *Fuel* **2016**, *163*, 122–128. [CrossRef]
29. Guan, L.; Yuan, Z.; Gu, Z.; Yang, L.; Zhong, W.; Wu, Y.; Sun, Sh.; Gu, C. Numerical simulation of ash particle deposition characteristics on the granular surface of a randomly packed granular filter. *Powder Technol.* **2017**, *314*, 78–88. [CrossRef]
30. Wang, F.L.; He, Y.L.; Tang, S.Z.; Kulacki, F.A.; Tao, Y.B. Particle filtration characteristics of typical packing granular filters used in hot gas clean-up. *Fuel* **2018**, *234*, 9–19. [CrossRef]
31. Wang, F.L.; He, Y.L.; Tang, S.Z.; Kulacki, F.A.; Tao, Y.B. Real-time particle filtration of granular filters for hot gas clean-up. *Fuel* **2019**, *237*, 308–319. [CrossRef]
32. Chen, J.; Li, X.; Huai, X.; Wang, Y.; Zhou, J. Numerical study of collection efficiency and heat-transfer characteristics of packed granular filter. *Particuology* **2019**, *46*, 75–82. [CrossRef]
33. Yang, J.; Bu, S.; Dong, Q.; Wu, J.; Wang, Q. Experimental study of flow transitions in random packed beds with low tube to particle diameter ratios. *Exp. Therm. Fluid Sci.* **2015**, *66*, 117–126. [CrossRef]
34. Freund, H.; Zeiser, T.; Huber, F.; Klemm, E.; Brenner, G.; Durst, F.; Emig, G. Numerical simulations of single phase reacting flows in randomly packed fixed-bed reactors and experimental validation. *Chem. Eng. Sci.* **2003**, *58*, 903–910. [CrossRef]
35. Gunjal, P.R.; Ranade, V.V. Modeling of laboratory and commercial scale hydro-processing reactors using CFD. *Chem. Eng. Sci.* **2007**, *62*, 5512–5526. [CrossRef]
36. Gunjal, P.R.; Kashid, M.N.; Ranade, V.V.; Chaudhari, R.V. Hydrodynamics of trickle-bed reactors: Experiments and CFD modeling. *Ind. Eng. Chem. Res.* **2005**, *44*, 6278–6294. [CrossRef]
37. Gunjal, P.R.; Ranade, V.V.; Chaudhari, R.V. Computational study of a single-phase flow in packed beds of spheres. *AIChE J.* **2005**, *51*, 365–378. [CrossRef]
38. Ranade, V.V. *Computational Flow Modeling for Chemical Reactor Engineering*; Academic Press: San Diego, CA, USA, 2002; 452p.
39. Cundall, P.A.; Strack, O.D. A discrete numerical model for granular assemblies. *Geotechnique* **1979**, *29*, 47–65. [CrossRef]
40. Shire, T.; O'Sullivan, C. Constriction size distributions of granular filters: A numerical study. *Geotechnique* **2016**, *66*, 826–839. [CrossRef]
41. Zhang, H.; Li, S. DEM simulation of wet granular-fluid flows in spouted beds: Numerical studies and experimental verifications. *Powder Technol.* **2017**, *318*, 337–349. [CrossRef]
42. Kh, A.B.; Mirghasemi, A.A.; Mohammadi, S. Numerical simulation of particle breakage of angular particles using combined DEM and FEM. *Powder Technol.* **2011**, *205*, 15–29.

43. Santos, D.A.; Barrozo, M.A.; Duarte, C.R.; Weigler, F.; Mellmann, J. Investigation of particle dynamics in a rotary drum by means of experiments and numerical simulations using DEM. *Adv. Powder Technol.* **2016**, *27*, 692–703. [CrossRef]
44. Khan, H.J.; Mirabolghasemi, M.S.; Yang, H.; Prodanović, M.; DiCarlo, D.A.; Balhoff, M.T. Study of formation damage caused by retention of bi-dispersed particles using combined pore-scale simulations and particle flooding experiments. *J. Pet. Sci. Eng.* **2017**, *158*, 293–308. [CrossRef]
45. Guo, Y.; Wassgren, C.; Ketterhagen, W.; Hancock, B.; James, B.; Curtis, J. A numerical study of granular shear flows of rod-like particles using the discrete element method. *J. Fluid Mech.* **2012**, *713*, 1–26. [CrossRef]
46. He, Y.; Bayly, A.E.; Hassanpour, A.; Muller, F.; Wu, K.; Yang, D. A GPU-based coupled SPH-DEM method for particle-fluid flow with free surfaces. *Powder Technol.* **2018**, *338*, 548–562. [CrossRef]
47. Guo, Y.; Curtis, J.S. Discrete element method simulations for complex granular flows. *Annu. Rev. Fluid Mech.* **2015**, *47*, 21–46. [CrossRef]
48. Shams, A.; Roelofs, F.; Komen, E.M.J.; Baglietto, E. Large eddy simulation of a nuclear pebble bed configuration. *Nucl. Eng. Des.* **2013**, *261*, 10–19. [CrossRef]
49. Matuttis, H.G. Simulation of the pressure distribution under a two-dimensional heap of polygonal particles. *Granul. Matter* **1998**, *1*, 83–91. [CrossRef]
50. Matuttis, H.G.; Luding, S.; Herrmann, H.J. Discrete element simulations of dense packings and heaps made of spherical and non-spherical particles. *Powder Technol.* **2000**, *109*, 278–292. [CrossRef]
51. Lu, G.; Third, J.R.; Müller, C.R. Discrete element models for non-spherical particle systems: From theoretical developments to applications. *Chem. Eng. Sci.* **2015**, *127*, 425–465. [CrossRef]
52. Zhu, J.; Liang, Y.; Zhou, Y. The effect of the particle aspect ratio on the pressure at the bottom of sandpiles. *Powder Technol.* **2013**, *234*, 37–45. [CrossRef]
53. Zhou, Z.Y.; Zou, R.P.; Pinson, D.; Yu, A.B. Angle of repose and stress distribution of sandpiles formed with ellipsoidal particles. *Granul. Matter* **2014**, *16*, 695–709. [CrossRef]
54. Van Buijtenen, M.S.; Buist, K.; Deen, N.G.; Kuipers, J.A.M.; Leadbeater, T.; Parker, D.J. Numerical and experimental study on spout elevation in spout-fluidized beds. *AIChE J.* **2012**, *58*, 2524–2535. [CrossRef]
55. Yu, Y.-S.; Tao, Y.-B.; He, Y.; He, Y.-L. Structure optimization of granular bed filter for industrial flue gas filtration containing coagulative particles: An experimental and numerical study. *Adv. Powder Technol.* **2020**, *31*, 2244–2256. [CrossRef]
56. Wang, F.-L.; Tang, S.-Z.; He, Y.-L.; Kulacki, F.A.; Tao, Y.-B. Parameter study of filtration characteristics of granular filters for hot gas clean-up. *Powder Technol.* **2019**, *353*, 267–275. [CrossRef]
57. Yu, Y.-S.; Tao, Y.-B.; Wang, F.-L.; Chen, X.; He, Y-L. Filtration performance of the granular bed filter used for industrial flue gas purification: A review of simulation and experiment. *Sep. Purif. Technol.* **2020**, *251*, 117318. [CrossRef]
58. Cheng, H.; Shuku, T.; Thoeni, K.; Tempone, P.; Luding, S.; Magnanimo, V. An iterative Bayesian filtering framework for fast and automated calibration of DEM models. *Comput. Methods Appl. Mech. Eng.* **2019**, *350*, 268–294. [CrossRef]
59. Benyahia, F.; O'Neill, K.E. Enhanced voidage correlations for packed beds of various particle shapes and sizes. *Part. Sci. Technol.* **2005**, *23*, 169–177. [CrossRef]
60. Gosman, A.D.; Ioannides, E. Aspects of computer simulation of liquid-fuelled combustors. *J. Energy* **1983**, *7*, 482–490. [CrossRef]
61. Hosseini, S.A.; Tafreshi, H.V. Modeling particle filtration in disordered 2-D domains: A comparison with cell models. *Sep. Purif. Technol.* **2010**, *74*, 160–169. [CrossRef]
62. Jin, X.; Yang, L.; Du, X. Modeling filtration performance of elliptical fibers with random distributions. *Adv. Powder Technol.* **2017**, *28*, 1193–1201. [CrossRef]
63. Ergun, S.; Orning, A.A. Fluid flow through randomly packed columns and fluidized beds. *Ind. Eng. Chem.* **1949**, *41*, 1179–1184. [CrossRef]
64. Eisfeld, B.; Schnitzlein, K. The influence of confining walls on the pressure drop in packed beds. *Chem. Eng. Sci.* **2001**, *56*, 4321–4329. [CrossRef]
65. Hinds, W.C. *Aerosol Technology Properties, Behavior, and Measurement of Airborne Particles*; John Wiley and Sons: Hoboken, NJ, USA, 1999; 504p.